Effect of salt on membrane protein Caveolin3 proved with NMR spectroscopy

Byoungduck Park[1] and Ji-Hun Kim[2]*

[1] College of Pharmacy, Sahmyook University, Seoul 01795, Republic of Korea
[2]College of Pharmacy, Chungbuk National University Cheongju, Chungbuk 28160, Republic of Korea

Abstract Caveolin3, mainly expressed in muscle tissue types, is a structural scaffolding protein of caveolae which are microdomains of plasma membrane. To elucidate the relationship between structure and function, several studies on the structure of caveolins using NMR have been reported. Because the ionic strength can affect the electrostatic-driven association of proteins with ligand and protein structure, the effect of salt in the structural studies has to be considered. In this work, we observed that the chemical shifts of Cav3 in the LPPG detergent change depending on salt concentration. The R2 values also show salt concentration-dependent changes. Specifically, in the N-terminal region where conformational changes and various interactions occur, the R2 values decrease. Interestingly, the R2 values of residues expected to be located in the LPPG detergent are also influenced by the salt concentration. This work suggests that the concentration of NaCl can affect interpretation of NMR data from membrane proteins.

Keywords Caveolin3, NMR, sodium chloride, relaxation, membrane protein

Introduction

Caveolae are the plasma membrane invaginations of 60-80 nm in diameter, enriched in cholesterol, glycosphingolipids, and lipid-anchored membrane proteins.[1, 2] They are observed in various mammalian cell types and participate in a wide variety of cellular processes, including endocytosis, cellular signaling, lipid metabolism, and mechanosensation.[3-6]

Caveolins are the scaffold proteins of caveolae, therefore, the family of caveolins has been the major biomarker of caveolae since their identification. The caveolin family consists of Caveolin1 (Cav1), Caveolin2 (Cav2), and Caveolin3 (Cav3).[7-9] Cav1, together with Cav2, is expressed in various tissues including adipocytes, and endothelial cells. On the other hand, Cav3 is predominantly expressed in skeletal and cardiac muscle tissue.[10] Their essential role is to form caveolae, but they are also known to play a variety of roles in various signaling pathways.[11, 12] In particular, some mutations in the residues of Cav3 are related to diseases such as limb-girdle muscular dystrophy (LGMD-1C), hyperCKemia, and rippling muscle disease (RMD).[13, 14] Thus, investigation of structural characteristics of Cav3 is important for understanding functional roles and its relation to human disease.

Cav3 is generally divided into four structural domains: a flexible N-terminal domain (residues 1-54), a scaffolding domain (res. 55-74), a membrane-embedded domain (res. 75-106), and a C-terminal cytosolic domain (res. 107-151).[15] The N-terminal

---

* Address correspondence to: **Ji-Hun Kim,** College of Pharmacy, Chungbuk National University, Chengju, Chungbuk 28160, Republic of Korea, Tel: 82-43-249-1343; Fax: 82-43-268-2732; E-mail: nmrjhkim@cbnu.ac.kr

domain contains a signature motif (FEDVIAEP) which is highly conserved among the caveolin family and a region undergoing pH-dependent conformational change.[15] In previous work, we revealed the complicated interplays within the N-terminal domain.[15] The scaffolding domain, which consists of helix, is essential to bind various other proteins. The membrane-embedded domain exhibits a helix-break-helix structure that penetrates membrane bilayers. The C-terminal domain composed of several helices possesses three cysteines where palmitoylation occurs.[16] Recently, the electron microscopy (EM) structure of Cav3 revealed that C-terminal domain plays a critical role in low molecular weight oligomerization.[17]

The process of protein folding is generally driven by forces arising from interactions within the protein itself as well as interactions with the solvent. Hydrophilic and hydrophobic forces critically contribute to these folding-related interactions. Furthermore, hydrophilic and hydrophobic contacts are also important for interactions with other proteins or ligands. Ionic strength in the solution can influence hydrophobic interactions as well as electrostatic-driven interactions, consequently, it affects the structure or interaction of the protein with others. Therefore, the salt effect must be considered in the studies on protein structure. In this work, we revealed that salt affects the structural properties of Cav3 in the LPPG detergent through the salt concentration-dependent changes of signals in the NMR spectra.

Experimental Methods

Expression and purification of Cav3 – A mutant form of Cav3 where six of the nine native cysteine residues were mutated to Ala or Ser (C19S, C72A, C94A, C98A, C124S, and C140S) was used in this work. The fifth, Cys site was mutated to Phe (C106), and sixth and eighth Cys sites (C116 and C129) were lipidated. This lipidated mutant, hereafter called Cav3^{5F68C}, was previously found to yield higher quality NMR spectra than any other Cav3 mutant. Expression, purification

of the Cav3 variant into LPPG micelles, and lipidation were carried out as previously described.[15, 18, 19] The summary of processes is briefly described as follows. Harvested cells, where Cav3^{5F68C} was highly expressed were resuspended in a lysis buffer (75 mM Tris, pH 7.8, 300 mM NaCl) containing 2 mM ethylenediaminetetraacetic acid (EDTA), 5 mM magnesium acetate, 2 mg/mL lysozyme, and 1 mM phenylmethylsulfonyl fluoride (PMSF). The resuspended mixture was tumbled for 90 min at room temperature, followed by sonication on ice. Inclusion bodies pelleted by centrifugation at 20,000 rpm for 30 minutes were solubilized in the buffer A (40 mM HEPES pH 7.8, 300 mM NaCl) containing 3% (v/v) N,N-Dimethyl-N-dodecylglycine betaine (Empigen, Sigma-Aldrich) detergent. Remained pellet was removed by centrifugation and the clarified soluble fraction was loaded into Ni-NTA resin column and sequentially washed with buffer A containing 3% (v/v) Empigen and buffer A containing 40 mM imidazole and 1.5% (v/v) Empigen for washing non-specific binding impurities from the resin. Subsequently, Empigen was replaced with 0.1% lyso-palmitoylphosphatidylglycerol (LPPG) by re-equilibrating the column with 20 column volumes of 20 mM sodium phosphate buffer (pH 7.2) supplemented with detergent. Cav3 was subsequently eluted from the column using 250 mM imidazole (pH 7.8) and 1 mM DTT. To lipidate Cav3^{5F68C}, 1.5 ml of Ellman's reagent (5,5' –dithio-bis-(2-nitrobenzoic acid) (DTNB) dissolved to a final concentration of 20 mM in 100 mM sodium phosphate buffer (pH 7.2) was mixed with 300-400 μL of a solution containing 1–2 mg of purified Cav3 in 250 mM imidazole buffer (pH 7.8, 1 mM EDTA and 2 mM DTT). Sixty microliters of a 100 mM EDTA (pH 7.2) stock solution was then added, and the total volume was adjusted to 3 ml with 20 mM sodium phosphate buffer (pH 7.2). The mixture was then tumbled for 4 hours at room temperature. To remove unreacted DTNB and free TNB, the sample was loaded on an Econo-Pac 10DG buffer exchange column, which was pre-equilibrated with 0.2% LPPG and 25 mM sodium phosphate buffer (pH 7.2). The TNB-modified protein was eluted in
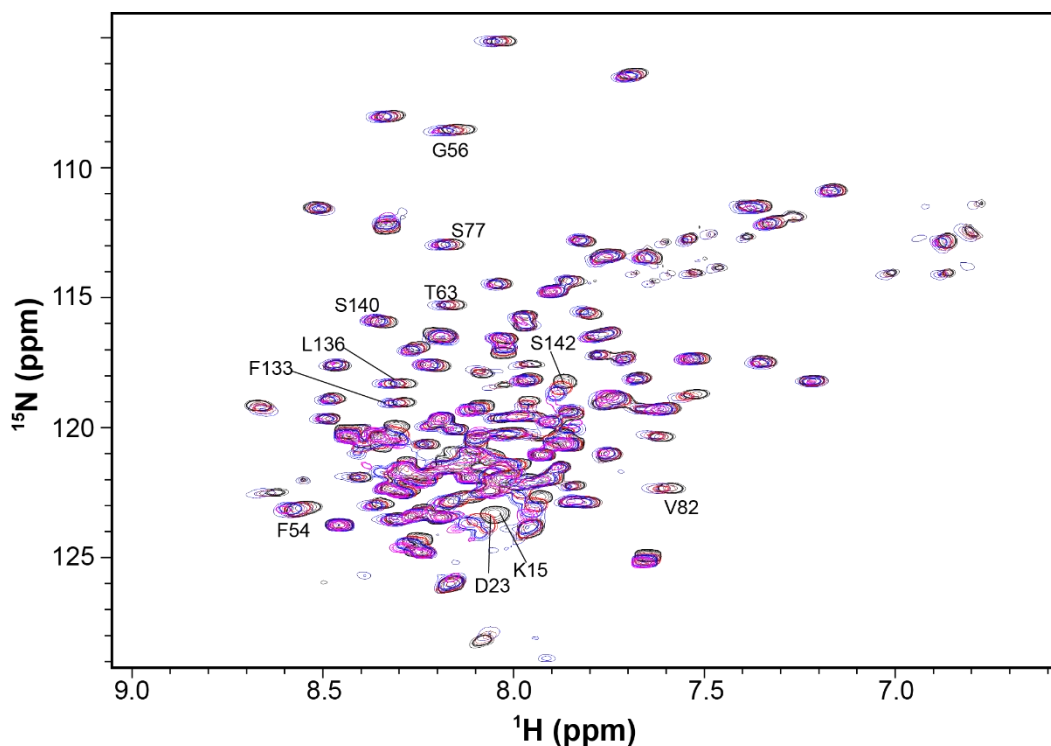
Figure 1. ^{1}H ^{15}N HSQC spectra of lipidated Cav3^{5F68C} in 100mM imidazole, pH 6.5, with various sodium chloride concentrations (black: 0 mM, red: 100 mM, blue: 200 mM, magenta: 400 mM NaCl) at 318K. The backbone amide cross peaks shown changes in the chemical shifts are annotated by residue names and numbers.

about 4 ml of buffer, and octanethiol was added to the elution pool to a final concentration of 10 mM followed by a 5 hours incubation. The mixture was then tumbled for 1 h with Ni-NTA resin equilibrated in 25 mM sodium phosphate buffer (pH 7.2). The resin was loaded into a column followed by washing and elution.

NMR spectra measurements – TROSY-HSQC and TROSY-based relaxation spectra were carried out at 45 °C on a Bruker 600 MHz NMR spectrometer equipped with cryoprobes. T2 values were measured from ^{1}H-^{15}N correlation spectra recorded with relaxation evolution delays of 17.28, 34.56, 51.84, 69.12, 86.4, 103.68, 138.24, 172.8 and 207.36 ms. A delay of 3.5 s was used between scans. To probe membrane topology, the 900 MHz ^{1}H^{15}N-TROSY spectrum of lipidated Cav3^{5F68C} was collected in the presence of lipophilic 16-doxylstearic acid (16-DSA)

at 45 °C. NMR samples contained concentrated lipidated Cav3^{5F68C} (200 uM final concentration) in a buffer containing 100 mM imidazole (pH 6.5), 1 mM EDTA, 5% (w/v) LPPG, 10% D$_2$O, with 4 mole % 16-DSA. To study the salt effect on lipidated Cav3^{5F68C}, ^{1}H^{15}N-TROSY spectra measured with NMR samples with indicated concentrations of sodium chloride on a Bruker 900 MHz NMR spectrometer equipped with cryoprobes. Spectra were processed using NMRPipe[20] and analyzed using Sparky[21].
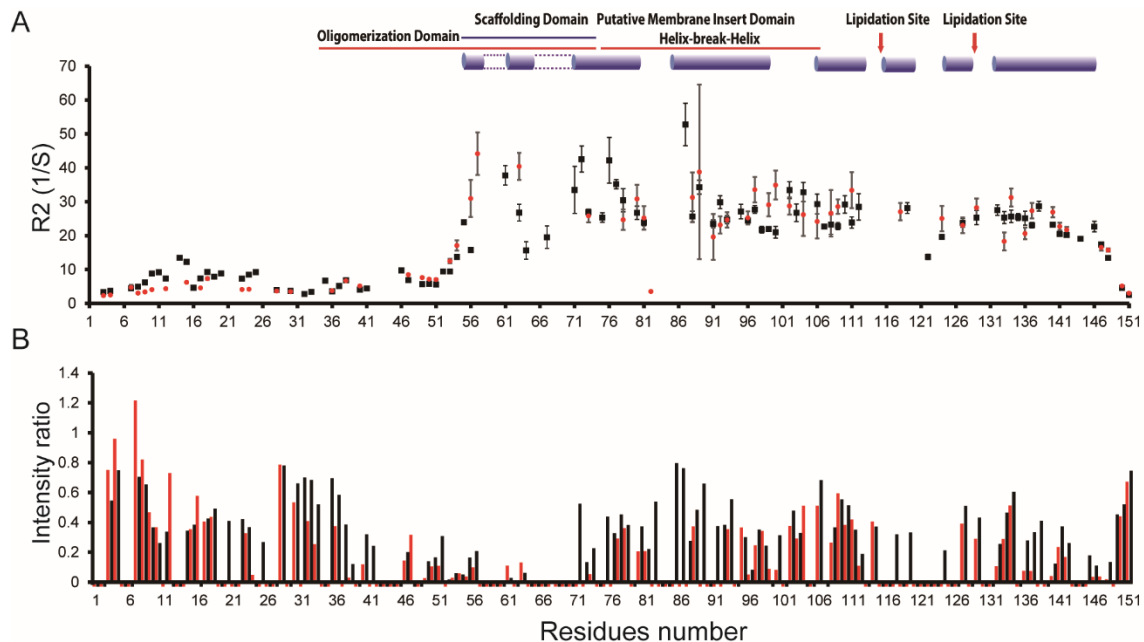
Results and Discussion

Salt titration of lipidated Cav3^{5F68C} – To probe the salt effect on integral membrane protein Cav3^{5F68C}, TROSY-HSQC spectra were collected in various concentrations of sodium chloride (Figure 1). For example, K15, D23, F54, G56, T63, S77, V82, F133,

L136, S140, and S142 undergo chemical shift changes. Interestingly, despite being an integral membrane protein, Cav3 exhibits chemical shift changes induced by sodium chloride that were not limited to the local region outside the membrane mimetics. In other words, membrane-associated residues are also affected by salt concentration, such as T63, S77, V82, F133, L136, S140, and S142. Considering that some peaks are unaffected by the salt concentration, it is believed that the position of the residue in the biological membrane is related to the extent to which it is affected by salt. Cav3 does not have the structure of the typical integral membrane protein. It is known that residues found in the deepest part of the membrane are located just in the middle of biological membranes. For that reason, salt has a global effect on the structure of Cav3 in the LPPG detergent.

Salt-mediated R2 and membrane topology changes –

To investigate the change of membrane topology and R2 values depending on the concentration of sodium chloride, transverse ^{15}N relaxation rates (R2) and paramagnetic relaxation enhancements of backbone amide resonances by the lipophilic paramagnetic probe, 16-DSA, were measured. Figure 2A reveals that R2 values of the N-terminal region (amino acids 8-16) decreased upon adding sodium chloride. These residues belong to the region where part of the N-terminal domain undergoes a pH-mediated topological rearrangement between soluble and membrane-anchored forms. Therefore, comparison of R2 values suggests that high salt reduces the population of the helical form at pH 6.5. Meanwhile, membrane-associated domain exhibits increased R2 values in the high salt condition, which indicates that scaffolding domain and membrane-insert domain go deeper into the detergent, consistent with the PRE results using 16-DSA in the Figure 2B.

Figure 2. Salt-mediated changes of R2 and membrane topology. (A) R2 values of Cav3^{5F68C} in the presence of 400 mM sodium chloride (red) or in the absence of salt (black) (B) The intensity of backbone amide peaks with the 4 mol % 16-DSA in the presence of 400 mM sodium chloride (red) or in the absence of salt (black). Negative peaks denote resonances for which the ratio could not be accurately determined.

Acknowledgements

References

1. D. A. Brown, E. London, *Annu Rev Cell Dev Biol* **14**, 111 (1998)
2. M. O. Parat, *Int Rev Cell Mol Biol* **273**, 117 (2009)
3. M. Bastiani, R. G. Parton, *J Cell Sci* **123**, 3831 (2010)
4. E. Gazzerro, F. Sotgia, C. Bruno, M. P. Lisanti, C. Minetti, *Eur J Hum Genet* **18**, 137 (2010)
5. C. Lamaze, N. Tardif, M. Dewulf, S. Vassilopoulos, C. M. Blouin, *Current opinion in cell biology* **47**, 117 (2017)
6. U. E. Martinez-Outschoorn, F. Sotgia, M. P. Lisanti, *Nat Rev Cancer* **15**, 225 (2015)
7. K. G. Rothberg, J. E. Heuser, W. C. Donzell, Y. S. Ying, J. R. Glenney, R. G. Anderson, *Cell* **68**, 673 (1992)
8. Z. Tang, P. E. Scherer, T. Okamoto, K. Song, C. Chu, D. S. Kohtz, I. Nishimoto, H. F. Lodish, M. P. Lisanti, *J Biol Chem* **271**, 2255 (1996)
9. P. E. Scherer, T. Okamoto, M. Chun, I. Nishimoto, H. F. Lodish, M. P. Lisanti, *Proc Natl Acad Sci U S A* **93**, 131 (1996)
10. T. M. Williams, M. P. Lisanti, *Ann Med* **36**, 584 (2004)
11. R. Baudrand, N. Gupta, A. E. Garza, A. Vaidya, J. A. Leopold, P. N. Hopkins, X. Jeunemaitre, C. Ferri, J. R. Romero, J. Williams, J. Loscalzo, G. K. Adler, G. H. Williams, L. H. Pojoga, *J Am Heart Assoc* **5**, (2016)
12. K. Mayurasakorn, N. Hasanah, T. Homma, M. Homma, I. K. Rangel, A. E. Garza, J. R. Romero, G. K. Adler, G. H. Williams, L. H. Pojoga, *Metabolism* **83**, 92 (2018)
13. Y. T. Horikawa, M. Panneerselvam, Y. Kawaraguchi, Y. M. Tsutsumi, S. S. Ali, R. C. Balijepalli, F. Murray, B. P. Head, I. R. Niesman, T. Rieg, V. Vallon, P. A. Insel, H. H. Patel, D. M. Roth, *J Am Coll Cardiol* **57**, 2273 (2011)
14. C. Minetti, F. Sotgia, C. Bruno, P. Scartezzini, P. Broda, M. Bado, E. Masetti, M. Mazzocco, A. Egeo, M. A. Donati, D. Volonte, F. Galbiati, G. Cordone, F. D. Bricarelli, M. P. Lisanti, F. Zara, *Nat Genet* **18**, 365 (1998)
15. J. H. Kim, J. P. Schlebach, Z. Lu, D. Peng, K. C. Reasoner, C. R. Sanders, *Biophys J* **110**, 2475 (2016)
16. Y. B. Ma, D. H. Kang, M. Kim, J. H. Kim, *J Korean Magn Reson* **23**, 67 (2019)
17. R. G. Parton, B. M. Collins, *Sci Adv* **8**, eabq6985 (2022)
18. D. W. Sim, Y. S. Lee, M. D. Seo, H. S. Won, J. H. Kim, *J Korean Magn Reson* **19**, 137 (2015)
19. J. H. Kim, D. Peng, J. P. Schlebach, A. Hadziselimovic, C. R. Sanders, *Biochemistry* **53**, 4320 (2014)
20. F. Delaglio, S. Grzesiek, G. W. Vuister, G. Zhu, J. Pfeifer, A. Bax, *J Biomol NMR* **6**, 277 (1995)
21. T. D. G. a. D. G. Kneller, SPARKY 3. University of California: San Francisco.